Analysis of acoustic energy and modes in a turbulent swirled combustor

By C. Martin†, L. Benoit†, F. Nicoud‡ AND T. Poinsot¶

This paper presents the analysis of the self-excited combustion instability encountered in a lab-scale, swirl-stabilised combustion system. The instability, successfully captured by reactive Large Eddy Simulation (LES) is used to verify an acoustic energy equation. This energy equation shows how the source term due to combustion (equivalent to the Rayleigh criterion) is balanced by the acoustic fluxes at the boundaries when reaching the limit cycle . Additionally, an Helmholtz-equation solver including flame-acoustics interaction modelling is used to predict the stability characteristics of the system. Feeding the flame-transfer function from the LES into this solver allows to predict an amplification rate for each mode. The unstable mode encountered in the LES compares well with the mode of the highest amplification factor in the Helmholtz-equation solver, as well in terms of mode shape as in frequency.

1. Introduction

During the design phases of modern combustion chambers for gas turbines, a critical problem is often encountered: combustion oscillations (Candel 1992; Crighton *et al.* 1992; Poinsot *et al.* 1987; Poinsot & Veynante 2001). These oscillations cannot be predicted at the design stage and correcting actions can be extremely costly at later stages. Testing burners in simplified combustion chambers is a common method to verify their stability but is also an ambiguous approach because it is known that a given burner can produce unstable combustion in one chamber and not in another. Methods which could provide stability analysis before any tests are therefore requested. This paper demonstrates that Large Eddy Simulation, coupled to acoustic analysis, can provide such information. A proper framework to analyse combustion stability is the wave equation for reacting flows (Poinsot & Veynante 2001). Such an equation is complex to derive because most assumptions used in classical acoustics must be revisited in a multi-species, non-isothermal, reacting gas. An approximate equation controlling the propagation of pressure perturbations in a reacting flow is:

$$\nabla \cdot \left(c_0^2 \nabla p_1\right) - \frac{\partial^2}{\partial t^2} p_1 = -(\gamma - 1)\frac{\partial \dot{\omega}_{T1}}{\partial t} - \gamma p_0 \nabla \vec{u}_1 : \nabla \vec{u}_1 \tag{1.1}$$

where the subscript 0 refers to mean quantities, and the subscript 1 to small perturbations. $\dot{\omega}_{T1}$ is the local perturbed heat release and c_0 is the sound speed, which can change locally because of changes in temperature and composition due to chemical reactions. These reactions are also the source of the additional RHS source term $(\gamma - 1)\partial\dot{\omega}_{T1}/\partial t$, which is responsible for combustion noise and instabilities. Equation (1.1) is difficult to use directly in practice. In the present work, it was solved or used in three different ways:

† CERFACS, CFD team, 42 Av. G. Coriolis, 31057 Toulouse Cedex
‡ Universite Montpellier II and CNRS
¶ IMF Toulouse, INP de Toulouse and CNRS UMR 5149, 31400 Toulouse CEDEX, France

• First, a fully compressible LES of the reacting flow was performed, in which the pressure perturbations p_1 are explicitely solved for using the full Navier-Stokes equation (not the linearized form of Eq. 1.1). The code used for this LES is described in section 2.

• Second, Eq. 1.1 is solved in the frequency domain by assuming mono-harmonic fluctuations. This is done using a Helmholtz tool described in Section 3.

• Third, Eq. 1.1 is integrated to derive an equation for the fluctuating energy. The definition of such an energy in a reacting flow is discussed in Section 4.

The reasons for this combined strategy are the following. First, it is now clear that Large Eddy Simulation (LES) is a powerful tool to study the dynamics of turbulent flames (see special issue of *Flow Turbulence and Combustion* (65, 2000) on LES of reacting flows or recent books on turbulent combustion: Peters 2000; Poinsot & Veynante 2001). Multiple recent papers have demonstrated the power of these methods (Angelberger, Egolfopoulos & Veynante 2000; Caraeni, Bergström & Fuchs 2000; Colin & Rudgyard 2000; Desjardins & Frankel 1999; Pierce & Moin 2004; Pitsch & Duchamp de la Geneste 2002 Selle *et al.* 2004). However, an important limitation of LES is its cost: the intrinsic nature of LES (full three-dimensional resolution of the unsteady Navier Stokes equations) makes it very expensive, even on today's computers. Faster tools are needed, for example for optimization and control of thermo-acoustic oscillations in chambers . Acoustic Helmholtz codes belong to this second category. These codes try to predict the global stability of a given combustion system by analyzing the amplification (or damping) of acoustic waves propagating through the entire combustion device. The most common versions of such codes describe combustion through very simplified linear formulations such as the n-tau model (Crocco 1969; Kaufmann, Nicoud & Poinsot 2002; Poinsot & Veynante 2001) or matrix formulations (Krueger *et al.* 2000; Paschereit, Flohr & Schuermans 2001; Polifke *et al.* 2001). In these formulations, the flame zone is viewed and modeled as a black box characterized only by its transfer function (or its matrix for matrix approaches), which essentially relates perturbations of heat release in the flame to perturbations of inlet velocity. LES and acoustic codes can be linked: LES is used to provide the mean fields, the unsteady fields and the flame transfer function. This flame transfer function can then be fed into acoustic codes to predict the overall stability of the combustion chamber when it is connected to upstream and downstream ducts.

2. Large Eddy Simulations for reacting flows in complex geometries

2.1. *Numerical methods for compressible reacting LES*

Most academic LES is often limited to fairly simple geometries for obvious reasons of cost and complexity reduction. In many cases, experiments are designed using simple two-dimensional shapes (Angelberger, Egolfopoulos & Veynante 2000; Duchamp de Lageneste & Pitsch 2001; Légier, Poinsot & Veynante 2000) or axisymmetrical configurations (Kempf *et al.* 2000; Pitsch & Steiner 2000) and simple regimes (low speed flows, fully premixed or fully non-premixed flames) to allow research to focus on the physics of the LES (subgrid scale models, flame/turbulence interaction model), and more generally, to demonstrate the validity of the LES concept in academic cases. This approach is clearly adequate in terms of modelling development, but it can also be misleading in various aspects when it comes dealing with complex flames in complex geometries, especially in real gas turbines for which specific problems arise:

• Real geometries cannot be meshed easily or rapidly with structured or block-structured meshes: up to now, most LES of reacting flows have been performed in combustion cham-

bers where structured meshes were sufficient to describe the geometry. This is no longer the case in gas turbines and this brings additional difficulties. Indeed, on structured meshes, building high-order spatial schemes (typically 4^{th} to 6^{th} order in space) is easy and provides very precise numerical methods (Ducros, Comte & Lesieur 1996; Gamet *et al.* 1999; Lele 1992). For complex geometries such structured meshes must be replaced by unstructured grids, on which constructing high-order schemes is a more difficult task.

- Unstructured meshes also raise a variety of new problems in terms of subgrid scale filtering: defining filter sizes on a highly anisotropic irregular grid is another open research issue (Sagaut 2000; Scotti, Meneveau & Fatica 1997; Scotti, Meneveau & Lilly 1993; Vasilyev, Lund & Moin 1998). Many LES models, developed and tuned on regular hexahedral grids may, perform poorly on the low-quality unstructured grids required to mesh real combustion chambers. For example, the filtered structure model (Ducros, Comte & Lesieur 1996) is difficult to extend to non structured grids.
- LES validation is often performed in laboratory low-speed unconfined flames, in which acoustics do not play a role and the Mach number remains small so that acoustics and compressibility effects can be omitted from the equations (low-Mach number approximation: Kempf *et al.* 2000; Pierce & Moin 2004). In most real flames (for example in gas turbines), the Mach number can reach much higher values and acoustics are important so that taking compressibility effects into account becomes mandatory. This leads to a significantly heavier computational task: since, acoustic waves propagate faster than the flow, the time step becomes smaller and the boundary conditions must handle acoustic wave reflections (Poinsot & Veynante 2001). Being able to preserve computational speed on a large number of processors then also becomes an issue simply to obtain a result in a finite time.
- At the present time, it is impossible to perform a true LES everywhere in the flow and it will remain so for a long time. For example, the flow between vanes in swirled burners, inside the ducts feeding dilution jets or through multiperforated plates would require too many grid points. Compromises must be sought to offer (at least) robustness in places where the grid is not sufficient to resolve the unsteady flow.

In the present work, the full compressible Navier Stokes equations are solved on hybrid (structured and unstructured) grids. Subgrid stresses are described by the WALE model (Nicoud & Ducros 1999). The flame/turbulence interaction is modeled by the Thickened Flame (TF) model (Angelberger, Egolfopoulos & Veynante 2000; Colin *et al.* 2000). The numerical scheme is explicit in time and provides third-order spatial and third-order time accuracy (Colin *et al.* 2000).

2.2. *Thickened Flame model and chemical scheme*

For this study, the standard TF model developed by Colin *et al.* (2000) is used: in this model, preexponential constants and transport coefficients are both modified to offer thicker reaction zones that can be resolved on LES meshes. The fundamental property justifying this approach has been put forward by Butler & O'Rourke (1977) by considering the balance equation for the k-species mass fraction Y_k in a one-dimensional flame of thermal thickness δ_L^0 and speed s_L^0:

$$\frac{\partial \rho Y_k}{\partial t} + \frac{\partial \rho u Y_k}{\partial x} = \frac{\partial}{\partial x}\left(\rho D_k \frac{\partial Y_k}{\partial x}\right) + \dot{\omega}_k(Y_j, T) \tag{2.1}$$

Modifying this equation to have:

$$\frac{\partial \rho Y_k^{th}}{\partial t} + \frac{\partial \rho u Y_k^{th}}{\partial x} = \frac{\partial}{\partial x}\left(\rho F D_k \frac{\partial Y_k^{th}}{\partial x}\right) + \frac{1}{F}\dot{\omega}_k\left(Y_j^{th}, T^{th}\right) \tag{2.2}$$

leads to a "thickened" flame equation where F is the thickening factor and superscript th stands for thickened quantities. Introducing the variable changes $X = x/F$; $\Theta = t/F$ leads to:

$$\frac{\partial \rho Y_k^{th}}{\partial \Theta} + \frac{\partial \rho u Y_k^{th}}{\partial X} = \frac{\partial}{\partial X}\left(\rho D_k \frac{\partial Y_k^{th}}{\partial X}\right) + \dot{\omega}_k\left(Y_j^{th}, T^{th}\right) \tag{2.3}$$

which has the same solution as Eq. (2.1) and propagates the flame front at the same speed s_L^0. However, $Y_k^{th}(x,t) = Y_k(x/F, t/F)$ shows that the flame is thickened by a factor F. The thickened flame thickness is $\delta_L^1 = F\delta_L^0$. Choosing sufficiently large values of F allows to obtain a thickened flame which can be resolved on the LES mesh. Typically, if n is the number of mesh points within the flame front (n is of the order of 5 to 10) and Δx the mesh size, the resolved flame thickness δ_L^1 is $n\Delta x$ so that F must be $F = n\Delta x/s_L^0$. Note that F is not an additional parameter of the model but is imposed by the previous relation as soon as the mesh is created. In the framework of LES, this approach has multiple advantages: when the flame is a laminar premixed front, the TF model propagates it, in the limit ot an infinitely thin front, at the laminar flame speed exactly like in a G equation approach. However, this flame propagation is due to the combination of diffusive and reactive terms which can also act independently so that quenching (near walls for example) or ignition may be simulated. Fully compressible equations may also be used as required to study combustion instabilities.

The thickening modification of the flame front also leads to a modified interaction between the turbulent flow and the flame: subgrid scale wrinkling must be reintroduced. This effect can be studied and parametrized using an efficiency function E derived from DNS results (Angelberger *et al.* 1998; Charlette, Veynante & Meneveau 2002; Colin *et al.* 2000). This efficiency function measures the subgrid scale wrinkling as a function of the local subgrid turbulent velocity u'_{Δ_e} and the filter width Δ_e. In practice, the diffusion coefficient D_k is replaced by EFD_k and the preexponential constant A by AE/F so that the conservation equation for species k is:

$$\frac{\partial \rho Y_k^{th}}{\partial t} + \frac{\partial \rho u Y_k^{th}}{\partial x} = \frac{\partial}{\partial x}\left(\rho E F D_k \frac{\partial Y_k^{th}}{\partial x}\right) + \frac{E}{F}\dot{\omega}_k\left(Y_j^{th}, T^{th}\right) \tag{2.4}$$

Such an equation propagates the turbulent flame at a turbulent speed $s_T = Es_L^0$, while keeping a thickness $\delta_L^1 = F\delta_L^0$. In laminar regions, E goes to unity, and Eq. 2.4 simply propagates the front at the laminar flame speed s_L^0. The subgrid scale wrinkling function E was obtained from the initial model of Colin *et al.* (2000) as a function of the local filter size Δ_e, the local subgrid scale turbulent velocity u'_{Δ_e}, the laminar flame speed s_L^0, the laminar and the flame thicknesses δ_L^0 and δ_L^1.

The TF model uses finite rate chemistry: here the configuration corresponds to a lean fully premixed flame so that a one-step Arrhenius kinetics is sufficient. This one-step scheme (called 1sCM1) has been fitted with a genetic algorithm based tool on a laminar flame structure. The reference mechanism used to fit 1sCM1 is the Peters propane scheme (Peters & Rogg 1993). 1sCM1 takes into account five species (C_3H_8,O_2, CO_2, H_2O and

Chemical parameters				Schmidt numbers				
A	$n^{C_3H_8}$	n^{O_2}	E_a	C_3H_8	O_2	CO_2	H_2O	N_2
$3.29E10$	0.856	0.503	31526	1.241	0.728	0.941	0.537	0.690

TABLE 1. Rate constants and Schmidt numbers for the 1sCM1 scheme: the activation energy is in cal/moles and the preexponential constants in cgs units.

N_2):

$$C_3H_8 + 5O_2 \longrightarrow 3CO_2 + 4H_2O \tag{2.5}$$

The rate of the single step reaction is given by:

$$q = A\left(\frac{\rho Y_{C_3H_8}}{W_{C_3H_8}}\right)^{n^{C_3H_8}}\left(\frac{\rho Y_{O_2}}{W_{O_2}}\right)^{n^{O_2}}\exp\left(-\frac{E_a}{RT}\right) \tag{2.6}$$

where the parameters are provided in Table 1.

The diffusion coefficient D_k of species k is obtained as $D_k = \nu/S_c^k$ where ν is the viscosity and S_c^k the fixed Schmidt number of species k. The Schmidt number values used in the present simulations are given in Table 1, and correspond to the PREMIX values measured in the burnt gases. The Prandtl number is set to 0.68. With this parameter set, the agreement between flame profiles obtained using AVBP or PREMIX with the same chemical scheme is excellent. The agreement between the Peters scheme and the 1sCM1 in terms of laminar flame speed is excellent for the lean up to stoechiometric mixtures.

3. Acoustic solver for the Helmholtz equation

The acoustic tool used in this study (called AVSP) solves the eigenvalue problem associated to the wave equation (1.1). When dealing with thermo-acoustic instabilities, it is current practice to model the geometry of the combustor by a network of 1D or 2D axisymmetric acoustic elements where a simplified form of Eq (1.1) can be solved (Poinsot & Veynante 2001; Stow & Dowling 2001). Jump relations are used to connect all these elements and the amplitude of the forward and backward acoustic waves are determined so that the boundary conditions are satisfied. The main drawback of this approach is that the geometrical details of a combustor cannot be accounted for and only the first "equivalent" longitudinal or orthoradial modes are sought for. In AVSP, a finite element strategy is used to discretize the exact geometry of the combustor so that no assumption is made a priori regarding the shape of the modes. This feature gives AVSP the potential to test the effect of (small) geometrical changes on the stability of the whole system.

The wave equation (1.1) is solved in the frequency domain by assuming harmonic variations at frequency $f = \omega/(2\pi)$ for pressure, velocity and local heat release perturbations ($i^2 = -1$):

$$p_1 = \hat{P}(x,y,z)\exp(-i\omega t), \quad \vec{u}_1 = \hat{u}(x,\vec{y},z)\exp(-i\omega t) \quad \text{and} \quad \dot{\omega}_{T1} = \hat{\Omega}_T\exp(-i\omega t) \tag{3.1}$$

Introducing Eq. (3.1) into Eq. (1.1) and neglecting the turbulent noise $\gamma p_0 \nabla \vec{u}_1 : \nabla \vec{u}_1$ in front of the combustion term $(\gamma-1)\partial\dot{\omega}_{T1}/\partial t$ leads to the Helmholtz equation:

$$\nabla \cdot \left(c_0^2 \nabla \hat{P}\right) + \omega^2 \hat{P} = i\omega(\gamma-1)\hat{\Omega}_T \tag{3.2}$$

where the unknown quantities are the complex amplitude $\hat{P}$ of the pressure oscillation at frequency f and pulsation ω. Note that $\hat{\Omega}_T$, the amplitude of the heat release perturbation is also unknown and must be modeled. This is obviously the difficult part of the modeling: it is done in AVSP through an extension of the $n-\tau$ model (Crocco 1969; Kaufmann, Nicoud & Poinsot 2002; Poinsot & Veynante 2001) where $\dot{\omega}_{T1} \propto n u_1(x_{\rm ref}, t-\tau)$. In 1D approaches, the interaction index n and time delay τ are two parameters describing the acoustic behaviour of a compact flame located at the axial position $x_{\rm ref}$. In AVSP, where the geometry of the combustor is fully described, the flame is distributed and the interaction index and time delay depend on space. These data can be extracted from LES results by post-processing either a self-excited or a forced oscillating regime. Once measured in LES, the fields $n(x)$ and $\tau(x)$ are used to model the unsteady heat release in Eq. (3.2) as $i\omega\hat{\Omega}_T = n(x) exp(i\omega\tau(x)) \nabla\hat{P}(x_{\rm ref}) \cdot \vec{n}_{\rm ref}/\rho_{\rm ref}$. Although they depend on ω in the most general case, n and τ have been obtained at the most energetic frequency observed in the LES ($f \simeq 380$ Hz) and considered constant over the frequency domain.

Three types of boundary conditions can be prescribed together with this equation ($\vec{n}$ is the outward unit normal vector to the boundary):

- Dirichlet condition, viz. $\hat{P} = 0$, on fully reflecting outlets,
- Neumann condition, viz. $\nabla\hat{P} \cdot \vec{n} = 0$, on fully rigid walls or reflecting inlets,
- Robin condition, viz. $cZ\nabla\hat{P} \cdot \vec{n} = i\omega\hat{P}$, on general boundaries, where Z is the local reduced complex impedance $Z = \hat{P}/\rho_0 c_0 \vec{\hat{u}} \cdot \vec{n}$

In this study, the reduced boundary impedance Z has been obtained by post-processing time series of the pressure and velocity on the boundary from the LES at $f \simeq 380$ Hz.

Knowing the boundary impedance (Z), the sound speed (c_0) distribution and the flame response $n(x);\tau(x)$, and assuming that Z does not depend on ω †, a Galerkin finite element method is used to transform Eq. (3.2) into a non-linear eigenvalue problem of size N (the number of nodes in the finite element grid used to discretize the geometry) of the form:

$$[A][\hat{P}] + \omega[B][\hat{P}] + \omega^2[C][\hat{P}] = [D(\omega)][\hat{P}] \tag{3.3}$$

where $[\hat{P}]$ stands for the column vector containing the eigenmode at pulsation ω, and $[A]$, $[B]$, $[C]$ are square matrices depending only on the disctretized geometry of the combustor. $[D(\omega)]$ is the unsteady contribution of the flame and depends on the pulsation through the combustion term $n(x)exp(i\omega\tau(x))$. No efficient numerical method exists to solve this non-linear eigenvalue problem. However, in the case where the unsteady flame response is neglected, viz. $[D(\omega)] = 0$, Eq. (3.3) simplifies into a quadratic eigenvalue problem depending only on ω and ω^2. A change of variable can then be used (Chatelin 1993) to obtain an equivalent linear eigen value problem of size $2 \times N$. Several numerical methods can then be used to assess the eigenmodes. Direct methods (e.g. QR-based) are exact and have the advantage to provide all the eigenmodes. However, they can be exp[ensive to solve for large problems ($N > 10^3$). Since only the first few frequencies are usually of interest from a physical point of view, it is more appropriate to use an iterative method which can be applied for large problems ($N > 10^5$) without difficulty. In AVSP, we are

† The same result holds if $1/Z = 1/Z_0 + C_1\omega + C_2/\omega$, where Z_0, Z_1 and Z_2 are complex valued constants.

using a parallel implementation of the Arnoldi method (Lehoucq *et al.* 1996), which enables to solve complex problems of size $N \simeq 20000$ in a few minutes.

Setting $[D(\omega)] = 0$ is equivalent to finding the eigenmodes of the burner, taking into account the presence of the flame through the mean temperature field but neglecting the flame effect as an acousticly active element. The boundary conditions are also considered for and this approximation can provide relevant information about the shape and real frequency of the first few modes of the combustor. However, since there is no coupling between the acoustics and the flame, there is no hope to discriminate between stable and unstable modes, which is the ultimate objective of this study. Under the assumption that the unsteady flame response acts as a small perturbation of the modes without combustion, a linear expansion technique can be developed to assess the imaginary part of ω, hence the stability of the perturbed modes (Benoit & Nicoud 2004; Nicoud & Benoit 2003). Another path has been followed in this study in order to handle cases where the unsteady response of the flame changes the modes significantly and when the linear expansion is not justified. The non-linear eigenvalue problem Eq. (3.3) is then solved iteratively, the k^{th} iteration consisting in solving the quadratic eigenvalue problem in ω_k defined as:

$$([A] - [D(\omega_{k-1})])\,[\hat{P}] + \omega_k[B][\hat{P}] + \omega_k^2[C][\hat{P}] = 0 \tag{3.4}$$

A natural initialization is to set $[D(\omega_0)] = 0$ so that the computation of the modes without combustion is in fact the first step of the iteration loop. Usually, less than 5 iterations are enough to converge towards the complex pulsation and associated mode.

This linearized approach to describe the stability of the burner in terms of modes has drawbacks but remains one of the basic tools to study instabilities:

- The linearization is valid only for small amplitude perturbations, a condition which is obviously not true when limit cycles typical of combustion instabilities are observed in gas turbines. However, this assumption is valid when the instability grows (Poinsot *et al.* 1988) and helps to determine the unstable modes: such modes have to appear and grow before they reach a limit cycle and any analysis adapted to this early phase is of interest.
- Most acoustic tools work on linear regimes for which each oscillatory mode is independent of other modes. Many combustion instabilities exhibit non-linear coupling where high-frequency modes couple with low-frequency oscillations: classical papers from Rogers & Marble (1956) mention such coupling. These were also observed in the experiment of Poinsot *et al.* (1987) in which a 530 Hz mode (often called rumble) was systematically accompanied by a high-frequency mode (called screech) at 3750 Hz. The fact that combustion instabilities involve more than one mode of oscillation is one of the basis of theories by Yang & Culick (1986). The tool presented above treats each mode individually and cannot simulate such phenomena.
- The description of the coupling between acoustics and combustion in such models is extremely crude. The response of the flame excited by an acoustic wave depends on several physical phenomena such as chemical reactions, species diffusion, vortex shedding, vortex-flame interaction, etc .... All these phenomena are not neglected in the present study but their cumulative effect is modeled through the global time scale τ and index n.

Despite these limitations, such tools are useful because they provide relevant information about the modes triggered by the acoustic/flame coupling while running fast: for the configuration described in section 5, only 8000 grid points were necessary to describe the geometry and obtain the first 4 modes. For comparison, half a million nodes were used to perfom the LES discussed in section 6. A typical run for solving the quadratic

eigenvalue problem of type Eq. (3.4) on this grid lasts 10 min by using 15 processors (R14000 500 MHz IP35) on an SGI O3800 parallel machine. Such tool can thus be used in the design process of new gas turbines to characterize their thermoacoustic modes. By describing the whole geometry between the compressor and the turbine, including all the injectors dispatched around the combustion chamber, such simulations would noticeably give unique information about the swirling modes that sometimes show up in large gas turbines. The difficult and computationally expensive task would be to compute the flame transfer function by performing a LES of the turbulent flame. Such simulation would be performed by considering an angular sector corresponding to only one injector, saving a huge amount of grid points and CPU resources.

4. Acoustic energy equation

The total acoustic energy equation is an integral form of the wave equation (1.1) which is quite useful to understand basic mechanisms of combustion instabilites. This equation cannot be used to predict unstable modes like the Helmholtz solver, but is a powerful method to analyze the results of an LES as done here. The conservation equation for the acoustic energy $e_1 = \frac{1}{2}\rho_0 u_1^2 + \frac{1}{2}p_1^2/(\rho_0 c_0^2)$ is derived in Poinsot & Veynante (2001) and can be written:

$$\frac{\partial e_1}{\partial t} = s_1 - \nabla \cdot (p_1 \vec{u}_1) \quad \text{with} \quad s_1 = \frac{(\gamma - 1)}{\gamma p_0} p_1 \dot{\omega}_{T1} \tag{4.1}$$

If integrated over the whole volume V of the combustor bounded by the surface A, it yields:

$$\frac{d}{dt}\int_V e_1 dV = \int_V s_1 dV - \int_A p_1 \vec{u}_1 . \vec{n} dA \text{ or } \frac{d}{dt}\mathcal{E}_1 = \mathcal{S}_1 - \mathcal{F}_1 \tag{4.2}$$

where $\vec{n}$ is the surface normal vector. This surface consists of walls or of inlet/outlet sections.

In Eq. (4.2), all terms are time dependent. The RHS source term $\mathcal{S}_1$ corresponds to the Rayleigh criterion (Rayleigh 1878): it measures the correlation between unsteady pressure p_1 and unsteady heat release $\dot{\omega}_{T1}$ averaged over the whole chamber. It can act as a source or a sink term for the acoustic energy. The other RHS term $\mathcal{F}_1$ is less studied because it is impossible to measure experimentally. It is an acoustic flux integrated on all the boundaries. Walls have zero contribution in this term because the velocity perturbations $\vec{u}_1$ vanish on walls. However, $\mathcal{F}_1$ may be large on inlets and outlets where it is usually a loss term. Eq. (4.1) is therefore a generalization of the Rayleigh criterion: the total acoustic energy in the chamber $\mathcal{E}_1$ will grow if the acoustic gain term $\mathcal{S}_1$ is larger than the acoustic losses $\mathcal{F}_1$. The magnitudes and relative importance of the two terms $\mathcal{S}_1$ and $\mathcal{F}_1$ are controversial issues in the field of combustion instabilities. For example, one important question is to know whether acoustic losses are important or not in the determination of limit cycles. For these limit cycles, the acoustic energy $\mathcal{E}_1$ must remain constant over a period of oscillations and Eq. (4.1) shows that such a cycle can be reached for two situations:

- The limit cycle may be *combustion controlled*: if the acoustic losses are small ($\mathcal{F}_1 = 0$), the pressure and heat release signals may adjust to give $\mathcal{S}_1 \simeq 0$. The limit cycle is reached when this phase shift leads to a zero Rayleigh term $\mathcal{S}_1$ as observed in certain experiments. Physically, this is often obtained when the heat release oscillations saturate (because the minimum reaction rate reaches zero at some instant of the cycle) or when the phase

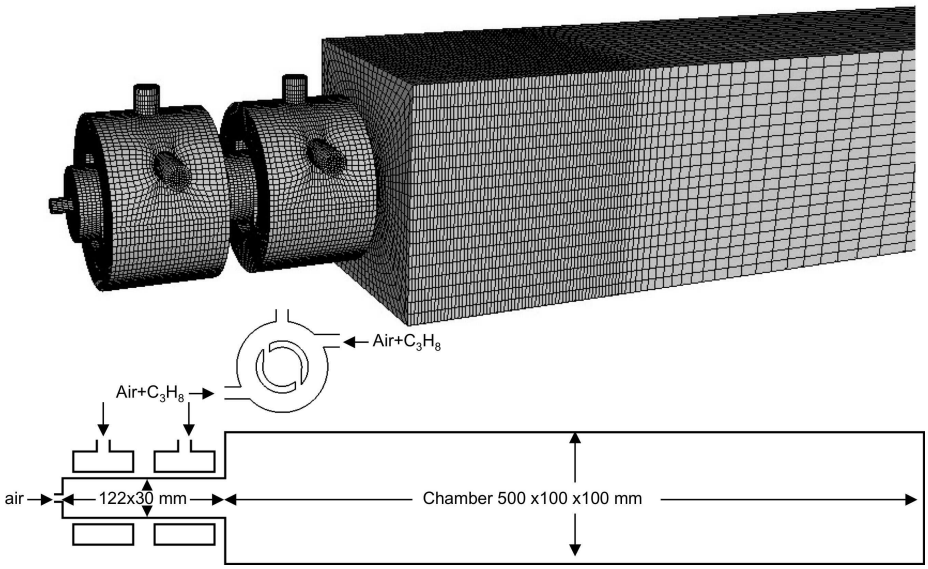

FIGURE 1. Configuration: a staged swirled combustor.

between pressure and heat release changes so that combustion itself controls the limit cycle amplitude.

• The limit cycle may be *acoustically controlled*: the source term $\mathcal{S}_1$ may be large (pressure and heat relase are oscillating in phase) but the acoustic losses are large too and compensate $\mathcal{S}_1$. In this case, the final amplitude of oscillation is controlled by the acoustic impedances of outlets and inlets.

Clearly, these two solutions lead to very different approaches of combustion instabilities: if the limit cycle is combustion controlled, the acoustic behavior of inlets and outlets have a limited effect on the stability; if it is acoustically controlled, acoustic impedances of inlets and outlets become essential elements of any method (experimental or numerical). In the present study, the LES results are post processed to measure all terms of Eq. (4.1) and determine whether the unstable mode is combustion or acoustically controlled (see Section 6.3).

5. Configuration

5.1. *Geometry: a swirled premixed combustor*

The methodologies described in the previous sections were tested for a swirled combustor displayed in Fig. 1. The configuration is typical of swirled combustion: premixed gases are introduced tangentially into a long cylindrical duct feeding the combustion chamber. The tangential injection creates the swirl required for stabilization. The fuel is propane. The two independant swirler elements allow fuel staging. The staging parameter α is defined as the ratio of fuel flow rate of the first to the second swirler. The regime studied here corresponds to the parameters given in Table 2. The staging of the burners corresponds to $\alpha = 0.3$.

Total flow rate (kg/s)	axial flow rate (kg/s)	Equivalence ratio	Reynolds number (burner mouth)
22.10^{-3}	4.10^{-3}	0.8	46700

TABLE 2. Flow parameters for combustion cases.

Case	Inlet σ	Outlet σ	Characteristic	Reduced impedance
LEAK	1000	1000	Non Reflecting outlet	$-0.85+0.35i$
REF	1000	10000	Reflecting outlet	$-0.04+0.21i$

TABLE 3. Acoustic inlet and outlet boundaries for the runs REF and LEAK. The last column comes from a post-processing of times series of velocity and pressure. The complex valued impedance was used as boundary condition in AVSP.

5.2. *Boundary conditions*

Specifying boundary conditions is a critical issue for compressible flows. Here, the NSCBC technique (Poinsot & Lele 1992; Poinsot & Veynante 2001) was used at the outlet. The level of reflection of this boundary can be controlled by changing the relaxation coefficient σ of the wave correction (Selle, Nicoud & Poinsot 2004), which determines the amplitude of the incoming wave L_1 entering the computational domain:

$$L_1 = \sigma(p - p_t) \tag{5.1}$$

where p_t is the prescribed pressure value at infinity. Eq. 5.1 acts on the flow like a spring mechanism with a stiffness σ. The impedance of the boundary is a function of σ which can be obtained analytically for simple case (Selle, Nicoud & Poinsot 2004). For more complex cases, this formula gives a good approximation of the actual impedance. For small values of σ, Eq. 5.1 keeps the pressure p close to its target value p_t while letting acoustic wave go out at the same time (Poinsot & Veynante 2001): the outlet is non reflecting. When large values of σ are used, the outlet pressure remains strictly equal to p_t and the outlet becomes totally reflecting. Two sets of computation will be shown (Table 3). The first one (called LEAK) corresponds to a case where the spring stiffness σ is small so that the outlet is non reflecting and the acoustic waves are evacuated with very small reflection levels.

For the second set (REF), σ is large and the outlet is reflecting (the pressure oscillation is almost zero).

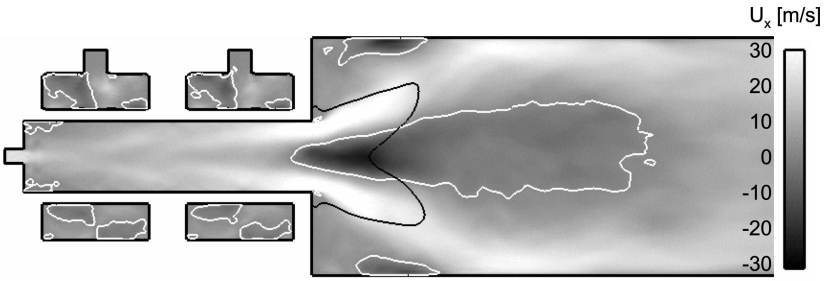

FIGURE 2. Mean axial velocity field, white line: iso-$u_x = 0$, black line: iso-T = 1500 K for stable combustion.

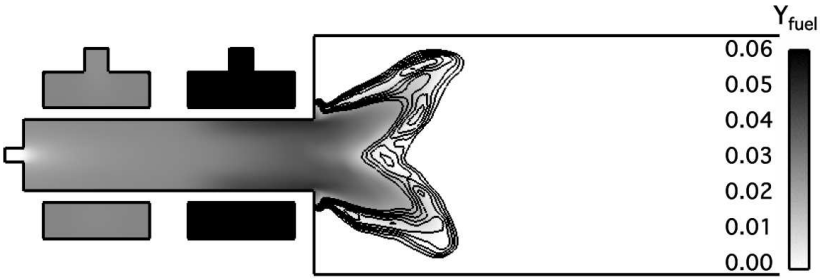

FIGURE 3. Mean fuel mass fraction field, black lines: iso-reaction rate for stable combustion.

6. Results

6.1. *Stable flow*

The first computation corresponds to the situation where the outlet section is non reflecting (case LEAK in Table 3). For this case, the acoustic feedback is minimized and the flame does not exhibit any strong unstable movement. The mean velocity and fuel mass fraction fields are displayed in Fig. 2 and Fig. 3. As expected, the downstream part of the central recirculation zone is filled by burnt gases and stabilize the turbulent flame.

6.2. *Acoustic analysis*

Using the mean temperature fields given by LES, the Helmholtz solver was used to obtain the thermoacoustic eigenmodes of the burner. For this analysis, the active effect of the flame is modelled using a transfer function ($n(x)$ and $\tau(x)$) obtained with LES, the mean sound speed is given by the average LES fields and the impedances of the REF run (Table 3) are used at the outlet and inlet of the combustor. When the outlet is set to a non reflecting condition similar to run LEAK, the acoustic solver predicts that all modes are damped. The frequency and decay/growth rate of the first four modes obtained with ($n(x)$ and $\tau(x)$ from LES) or without ($n(x)$ set to zero) acoustics/flame coupling in the REF case are displayed in Tab. 4. Note that the first four modes are mainly longitudinal. When the unsteady effect of the flame is not accounted for, all modes are damped (negative growth rate), because the mechanism which feeds the instability is not present and acoustic losses through the inlet/outlet boundary are not compensated. When the flame transfer function obtained from LES is used, the first mode is drastically damped by the acoustics/flame interaction, while the second mode is predicted to be the most unstable. The pressure node in the second mode vanishes when the acoustic/flame

Mode - no active flame	Frequency [Hz]	Growth rate $[rd.s^{-1}]$	Mode - active flame	Frequency [Hz]	Growth rate $[rd.s^{-1}]$
1	308	-42	1	304	-672
2	435	-23	2	432	653
3	833	-3.1	3	835	5
4	1184	-63	4	1136	232

TABLE 4. AVSP results: frequencies and growth rates of the first four modes predicted by the acoustic solver with and without acoustics/flame coupling.

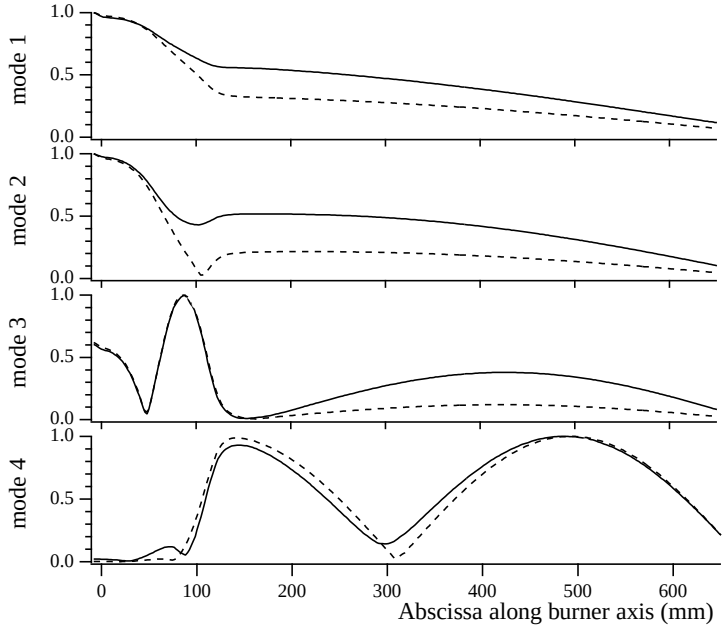

FIGURE 4. Longitudinal structure of the first four modes obtained with acoustic analysis: Normalized p_1^{rms} evolution along burner axis with acoustics/flame coupling (——) and without (- - - -).

interaction is taken into acount. The 3^{rd} and 4^{th} modes are only marginally triggered. Recall however that the flame transfer function has been assessed by post-processing the LES results in the 400 Hz range so that it is not clear whether the acoustics/flame interaction is properly accounted for as far as modes in the 1000 Hz range are concerned. Still, accounting for the flame transfer function allowed to discriminate between the first two modes of the burner although neither big difference in their shape can be found in Fig. 4 nor clear frequency discrimination can be stated compared to LES results (380 Hz).

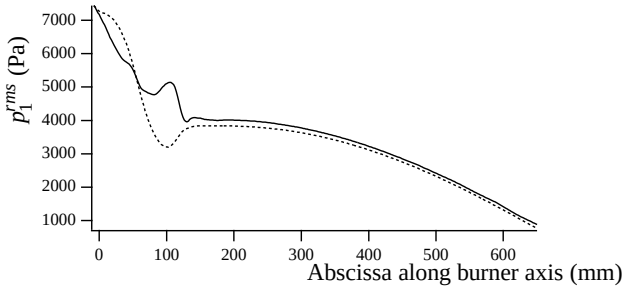

FIGURE 5. Comparison of LES (———) and acoustic (- - - -) solvers: RMS pressure fluctuations p_1^{rms} along burner axis.

6.3. *LES results*

In addition to the average results of Section 6.1, LES also reveals that the combustor can exhibit a strong unstable mode when the outlet is acoustically closed (case REF). In this case, soon after ignition, the pressure and the global heat release start oscillating (Fig. 6 a) at 380 Hz which is very close to the mode predicted by AVSP in Section 6.2. To analyse the behavior of this instability, the following sequence is set up:

- Starting from a stable flame (LEAK), the outlet impedance is changed to become reflecting (case REF) at time $t = 0.127s$ (Fig. 6). The oscillation grows and reaches a limit cycle at a frequency of 380 Hz mode which is close to mode 2 predicted by the Helmholtz code (Section 6.2) at 432 Hz. Its mode structure is also very well predicted (Fig. 5): the pressure perturbation p_1^{rms} measured in the LES matches the acoustic structure of the 432 Hz mode predicted by AVSP.
- At time $t = 0.173s$, the outlet impedance is switched again to a non reflecting condition (case LEAK) so that the instability disappears.

This scenario provides three phases which are studied sequentially:

- A linear growth between times $0.127s$ and $0.150s$ (Section 6.4),
- A limit cycle between times $0.150s$ and $0.173s$ (Section 6.5),
- A decay phase starting at $t = 0.173s$ (Section 6.6)

For each phase, the instability is analyzed in terms of flame shape, flame oscillation and phase between heat release and pressure. Moreover, the acoustic energy equation budget is closed and all terms are analyzed.

6.4. *Growth phase*

Once the outlet boundary is acoustically closed (t= 0.127 s), the thermoacoustic instability starts. Fig. 6 displays the time variations of the combustion source term $\mathcal{S}_1$, the acoustic losses $\mathcal{F}_1$ (Fig. 6 b), the total acoustic energy in the chamber $\mathcal{E}_1$ (Fig. 6 d) and shows that the budget of Eq. 4.2 is very well closed by the LES data: the difference $\mathcal{S}_1 - \mathcal{F}_1$ matches the time derivative of $\mathcal{E}_1$ (Fig. 6 c). This validates both the LES results and the wave equation 4.2. It is also the first example of such a treatment for a resonating combustor. Since the budget is closed, individual terms can then be analyzed.

The phase angle between pressure and heat release is displayed in Fig. 6a. During the growth phase, it is close to zero and slowly shifting towards $\pi/4$, leading to a strong coupling between pressure and heat release i.e. a positive S_1 term. During the growth phase, the source term S_1 is large and always positive (Fig. 6 b), because the phase angle stays in the $[-\pi/2;\pi/2]$ range. Fig. 6 b shows clearly that the acoustic losses balance the reacting term S_1 in the acoustic buget equation.

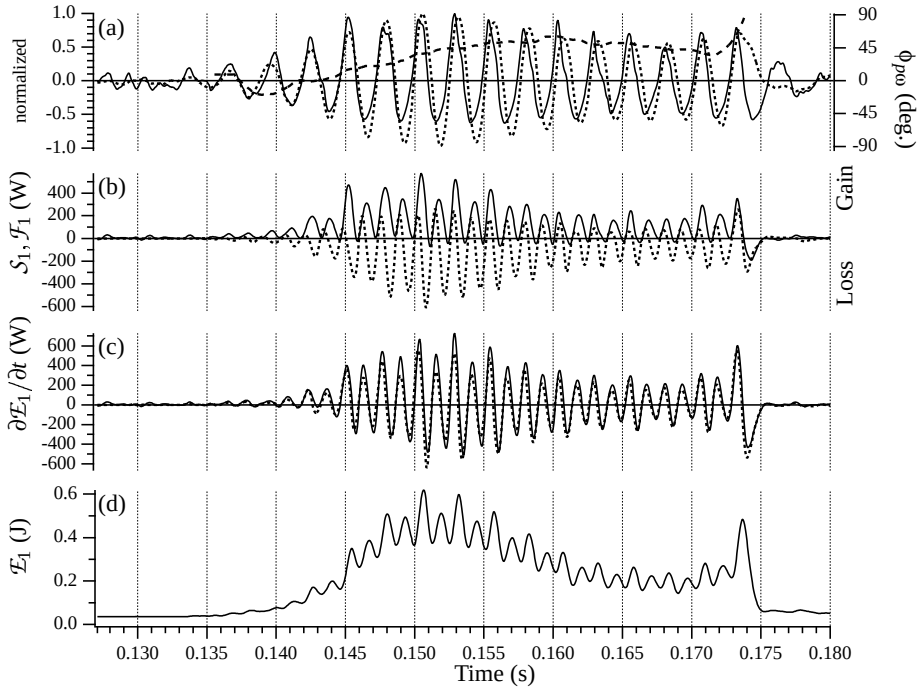

FIGURE 6. Closure of the acoustic energy equation: (a) mean normalized value of pressure (———), heat release (·····) and phase angle between these signals (– – – –); (b) $\mathcal{S}_1$ (———) and $\mathcal{F}_1$ (·····); (c) $\mathcal{S}_1 - \mathcal{F}_1$ (———) and $\partial\mathcal{E}_1/\partial t$ (·····); (d) $\mathcal{E}_1$.

6.5. *Limit cycle*

At t=0.150s, the instability reaches a limit cycle at 380 Hz. Before reaching this limit cycle, a large overshoot of acoustic energy is observed: this is typical of combustion instabilities and it has been observed experimentally. Fig. 6 shows that reaching the non-linear zone, the phase difference between pressure and heat release increases from zero to $\pi/4$ in the limit cycle zone. The drift of this phase difference together with increasing acoustic losses lead to the saturation of the instability.

The coupling loop between p_1 and $\dot{\omega}_{T1}$ can be identified from LES as follows. The longitudinal mode induces the formation of a vortex ring at the dump plane. This vortex ring strongly interacts in phase with the flame. Fig. 7 illustrates the interaction between the acoustically induced vortex ring and the flame brush. Fig. 8 allows to locate LES snapshots in the acoustic period and displays the mean pressure fluctuation p_1 in the flame zone, the heat release fluctuation $\dot{\omega}_{T1}$, and the fluctuation of the mean velocity in the dump plane u_1^{dump}. At instant 1, a vortex ring appears at the dump plane when du_1^{dump}/dt is maximum. The ring structure detaches and is convected through the flame by the mean flow (instants 2, 3 and 4). During the period 1-3 the flow incoming from the injector pipe stretches the flame, increasing its area, whereas the flame wrinkling by the vortex ring remains weak. Consequently $\dot{\omega}_{T1}$ increases with a medium slope. Between points 3 and 5 the vortex ring is clearly wrinkling the flame and $\dot{\omega}_{T1}$ increases faster. Moreover, the vortex ring is gradually destroyed, and its global coherence disappears between instants 4 and 5, at a moment when du_1^{dump}/dt is minimum. At instant 5 some

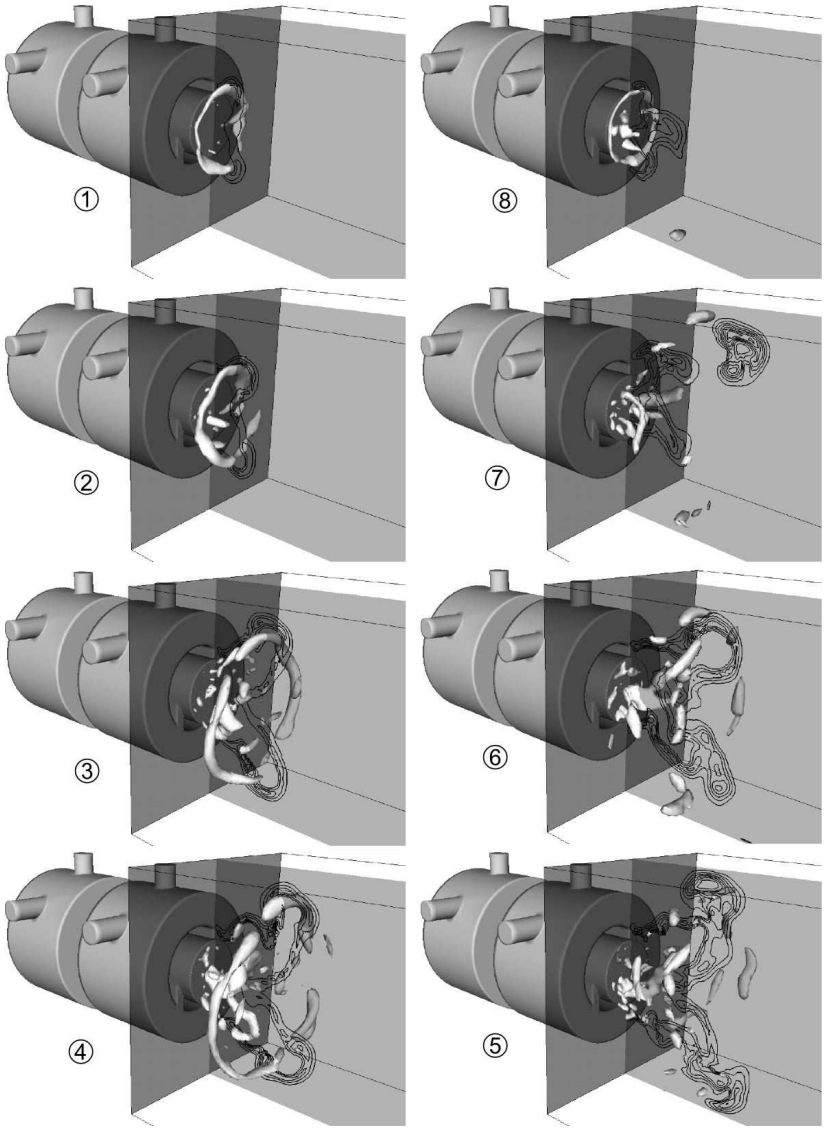

FIGURE 7. Vortex ring shedding for a period during the limit cycle, isosurface: Q vortex criterion; black lines: iso-reaction rate.

coherent structures are still interacting with the flame, producing (noisy) flame pockets and cusps. After 5, the flame burns out the fresh gases present in the chamber and propagates back to the injection pipe decreasing the overall flame surface and $\dot{\omega}_{T1}$.

6.6. *Decay phase*

The decay phase is triggered by the sudden change in the acoustic outlet boundary condition switching to non-reflecting (LEAK). The phase angle $\phi_{p\omega}$ increases by a large amount: $\phi_{p\omega} > \pi/2$ at $t = 0.174s$ i.e $1.2ms$ after relaxing outlet pressure (Fig. 6). At this time $\mathcal{S}_1$ becomes globally negative for the first time and the instability is rapidly damped. The acoustic losses actually become positive (gain term) during this last oscilation but

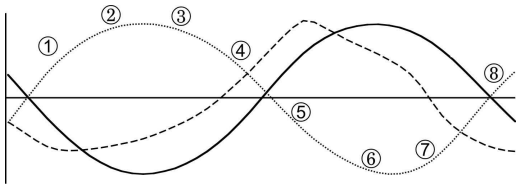

FIGURE 8. Time signals during the limit cycle and snapshots corresponding to the previous figure: pressure (———), inlet velocity (– – – –) and total heat release (·····)

the instability *engine* is broken and the Rayleigh term $\mathcal{S}_1$ becomes negative during a half cycle ($0.173 < t < 0.175ms$ on Fig. 6) leading to the immediate disappearance of all unstable activity.

7. Conclusions

Three complementary tools have been used to analyse the instability modes of a staged swirled combustor: full compressible LES, Helmholtz analysis and budget of acoustic energy. The two latter methods utilize LES results but provide essential new elements: the Helmholtz results allow the exact identification of modes appearing during the instability, while the budget of acoustic energy demonstrates that the Rayleigh criterion is not the only or even the largest term in the acoustic energy equation: acoustic losses at the outlet of the combustor contribute significantly to the budget of acoustic energy and determine the levels of oscillation amplitudes as well as their appearance.

Acknowledgments

Certain numerical simulations have been conducted on the computers of the CINES and IDRIS French national computing centers. Simulations have been supported partly by ALSTOM POWER and by the EC program (WP2) FUELCHIEF.

REFERENCES

ANGELBERGER, C., EGOLFOPOULOS, F. & VEYNANTE, D. 2000 Large Eddy Simulations of chemical and acoustic effects on combustion instabilities *Flow Turb. and Combustion* **65**, 205-22.

ANGELBERGER, D., VEYNANTE, D., EGOLFOPOULOS, F. & POINSOT, T. 1998 Large Eddy Simulations of combustion instabilities in premixed flames *Summer Program* 61-82.

BENOIT, L. & NICOUD, F. 2004 Numerical assessment of thermo-acoustic instabilities in gas turbines *ICFD Conference of numerical methods for fluid dynamics.*

BUTLER, T.D. & O'ROURKE, P.J. 1977 A numerical method for two-dimensional unsteady reacting flows *16th Symp. (Int.) on Combustion* 1503 - 1515.

CANDEL, S. 1992 Combustion instabilities coupled by pressure waves and their active control. *24th Symp. (Int.) on Combustion* 1277-1296.

CARAENI, D., BERGSTRÖM, C. & FUCHS, L. 2000 Modeling of Liquid Fuel Injection, Evaporation and Mixing in a Gas Turbine Burner Using Large Eddy Simulation *Flow Turb. and Combustion* **65**, 223-244.

CHARLETTE, F., VEYNANTE, D. & MENEVEAU, C. 2002 A power-law wrinkling model

for LES of premixed turbulent combustion: Part I - non-dynamic formulation and initial tests *Combust. Flame* **131**, 159-180.

CHATELIN, F. 1993 Eigenvalues of matrices, J. Wiley.

COLIN, O. & RUDGYARD, M. 2000 Development of high-order Taylor-Galerkin schemes for unsteady calculations *J. Comput. Phys.* **162**, 338-371.

COLIN, O., DUCROS, F., VEYNANTE, D. & POINSOT, T. 2000 A thickened flame model for large eddy simulations of turbulent premixed combustion *Phys. Fluids* **12**, 1843-1863.

CRIGHTON, D.G., DOWLING, A., FFOWCS WILLIAMS, J.E:, HECKL, M. & LEPPINGTON, F. 1992 Modern methods in analytical acoustics, Springer Verlag.

CROCCO, L. 1969 Research on combustion instability in liquid propellant rockets. *12th Symp. (Int.) on Combustion* 85-99.

DESJARDINS, P.E. & FRANKEL, S.H. 1999 Two dimensional Large Eddy Simulation of soot formation in the near field of a strongly radiating nonpremixed acetylene-air jet flame *Combust. Flame* **119**, 121-133.

DUCHAMP DE LAGENESTE, L. & PITSCH, H. 2001 Progress in large eddy simulation of premixed and partially premixed turbulent combustion *Annual Research Briefs* 61-82.

DUCROS, F., COMTE, P. & LESIEUR, M. 1996 Large-eddy simulation of transition to turbulence in a boundary layer developing spatially over a flat plate *J. Fluid Mech.* **326**, 1-36.

GAMET, L., DUCROS, F., NICOUD, F. & POINSOT, T. 1999 Compact Finite Difference Schemes on Non-Uniform Meshes. Application to Direct Numerical Simulations of Compressible Flows. *Int. J. for Num. Meth. in Fluids* **29**, 159-191.

KAUFMANN, A., NICOUD, F. & POINSOT, T. 2002 Flow forcing techniques for numerical simulation of combustion instabilities *Combust. Flame* **131**, 371-385.

KELLER, J.O., VANEVELD, L., KORSCHELT, D., HUBBARD, G.L., GHONIEM, A.F., DAILY, J.W. & OPPENHEIM, A.K. 1981 Mechanism of instabilities in turbulent combustion leading to flashback *AIAA Journal* **20**, 254-262.

KEMPF, A., FORKEL, H., CHEN, J.-Y., SADIKI, A. & JANICKA, J. 2000 Large-eddy simulation of a counterflow configuration with and without combustion *Proc. of the Combustion Institute* **28**, 35-40.

KRUEGER, U., HUEREN, J., HOFFMANN, S., KREBS, W., FLOHR, P. & BOHN, D. 2000 Prediction and measurements of thermoacoustic improvements in gas turbines with annular combustion systems *ASME TURBO EXPO 2000* 2000-GT-0095, ASME Paper,

LEHOUCQ, R., MASCHOFF, K., SORENSEN, D. & YANG, C. 1996 ARPACK website, http://www.caam.rice.edu/software/ARPACK.

LELE, S. 1992 Compact finite difference schemes with spectral like resolution *J. Comput. Phys.* **103**, 16-42.

LÉGIER, J.-PH., POINSOT, T. & VEYNANTE, D. 2000 Dynamically thickened flame Large Eddy Simulation model for premixed and non-premixed turbulent combustion *Summer Program 2000* 157-168.

NICOUD, F. & BENOIT, L. 2003 Global tools for thermo-acoustic instabilities in gas turbines *Bulletin of the American Physical Society* **48**, 240-241.

NICOUD, F. & DUCROS, F. 1999 Subgrid-scale stress modelling based on the square of the velocity gradient *Flow Turb. and Combustion* **62**, 183-200.

PASCHEREIT, C.O., FLOHR, P. & SCHUERMANS, B. 2001 Prediction of combustion oscillations in gas turbine combustors. *39th AIAA Aerospace Sciences Meeting and Exhibit.* 2001-0484, AIAA Paper, 484.

PETERS, N. 2000 Turbulent combustion, Cambridge University Press.

PETERS, N. & ROGG, B. 1993 Reduced Kinetic Mechanisms for Applications in Combustion Systems, Springer Verlag.

PIERCE, C.D. & MOIN, P. 2004 Progress-variable approach for large eddy simulation of non-premixed turbulent combustion *J. Fluid Mech.* **504**, 73-97.

PITSCH, H. & DUCHAMP DE LA GENESTE, L. 2002 Large Eddy Simulation of Premixed Turbulent Combustion using a level-set approach *Proc of the Comb. Institute* **29**, 2001-2008.

PITSCH, H. & STEINER, H. 2000 Large Eddy Simulation of a Turbulent Piloted Methane/Air Diffusion Flame (Sandia Flame D) *Phys. Fluids* **12**, 2541-2554.

POINSOT, T. & LELE, S. 1992 Boundary conditions for direct simulations of compressible viscous flows *J. Comput. Phys.* **101**, 104-129.

POINSOT, T., TROUVE, A., VEYNANTE, D., CANDEL, S. & ESPOSITO, E. 1987 Vortex driven acoustically coupled combustion instabilities *J. Fluid Mech.* **177**, 265-292.

POINSOT, T. & VEYNANTE, D. 2001 Theoretical and numerical combustion, R.T. Edwards.

POINSOT, T., VEYNANTE, D., BOURIENNE, F., CANDEL, S., ESPOSITO, E. & SURJET, J. 1988 Initiation and suppression of combustion instabilities by active control *22nd Symp. (Int.) on Combustion* 1363-1370.

POLIFKE, W., PONCET, A., PASCHEREIT, C.O. & DOEBBELING, K. 2001 Reconstruction of acoustic transfer matrices by instationnary computational fluid dynamics *J. Sound Vibration* **245**, 483-510.

RAYLEIGH, L. 1878 The explanation of certain acoustic phenomena *Nature* July 18, 319-321.

ROGERS, D.E. & MARBLE, F.E. 1956 A mechanism for high frequency oscillations in ramjet combustors and afterburners *Jet Propulsion* **26**, 456-462.

SAGAUT, P. 2000 Large Eddy Simulation for incompressible flows, Springer-Verlag.

SCOTTI, A., MENEVEAU, C. & FATICA, M. 1997 Generalized Smagorinski model for anisotropic grids *Phys. Fluids* **9**, 1856-1858.

SCOTTI, A., MENEVEAU, C. & LILLY, D.K. 1993 Generalized Smagorinski model for anisotropic grids *Phys. Fluids* **5**, 2306-2308.

SELLE, L., LARTIGUE, G., POINSOT, T., KOCH, R., SCHILDMACHER, K.U., KREBS, W., PRADE, B., KAUFMANN, P. & VEYNANTE, D. 2004 Compressible Large-Eddy Simulation of turbulent combustion in complex geometry on unstructured meshes *Combust. Flame* **137**, 489-505.

SELLE, L., NICOUD, F. & POINSOT, T. 2004 The actual impedance of non-reflecting boundary conditions: implications for the computation of resonators *AIAA Journal* **42**, 958-964.

STOW, S.R. & DOWLING, A.P. 2001 Thermoacoustic oscillations in an annular combustor *ASME Paper*

VASILYEV, O. V., LUND, T.S. & MOIN, P. 1998 A general class of commutative filters for LES in complex geometries *J. Comput. Phys.* **146**, 82-104.

YANG, V. & CULICK, F.E.C 1986 Analysis of low-frequency combustion instabilities in a laboratory ramjet combustor *Combust. Sci. Tech.* **45**, 1-25.